Mechanisms for Liquid Slip at Solid Surfaces

Seth Lichter,[1] Alex Roxin,[2,3] and Shreyas Mandre[1]

[1]*Department of Mechanical Engineering, Northwestern University, Evanston, Illinois 60208, USA*
[2]*Department of Engineering Science and Applied Mathematics, Northwestern University, Evanston, Illinois 60208, USA*
[3]*Neurophysics and Physiology of the Motor System, Université René Descartes, Paris, France*

(Received 17 February 2004; published 20 August 2004)

One of the oldest unresolved problems in fluid mechanics is the nature of liquid flow along solid surfaces. It is traditionally assumed that across the liquid-solid interface, liquid and solid speeds exactly match. However, recent observations document that on the molecular scale, liquids can slip relative to solids. We formulate a model in which the liquid dynamics are described by a stochastic differential-difference equation, related to the Frenkel-Kontorova equation. The model, in agreement with molecular dynamics simulations, reveals that slip occurs via two mechanisms: localized defect propagation and concurrent slip of large domains. Well-defined transitions occur between the two mechanisms.

DOI: 10.1103/PhysRevLett.93.086001 PACS numbers: 83.50.Lh, 05.45.–a, 47.90.+a, 68.08.–p

A century of macroscopic measurements on liquid flows has consistently confirmed the no-slip condition, which states that liquid and solid share the identical velocity tangential to a liquid-solid interface. However, Navier, who derived the equations for bulk fluid flow in 1823, proposed that fluids could slip relative to solid boundaries [1]. Navier's early study hinted that macroscopic measurements on liquid flows might conform to the no-slip prediction while admitting a small amount of slip. Contrary to macroscopic flows, a small amount of slip can have serious consequences for nanoscale flows, on the design of nanoscale flow devices and on our understanding of cellular-level biological flows [2]. Molecular-scale slip has now been inferred from observations using sensitive force measurements [3] and confirmed using visual techniques [4,5] and molecular dynamics (MD) simulation data [6–8]. We formulate a model that describes the molecular states of slip. The predictions of the model are compared with physical experiment, where these results are available. In general, though, comparison is made with MD computational experiments.

Our formulation accounts in a simplified manner for recent x-ray scattering, atomic-force microscopy, and other observations, which reveal that, near a solid substrate, the average liquid density passes through several local maxima and minima before settling to the bulk value [Fig. 1(a), black] [6,9,10]. In particular, a large peak in the density profile occurs between the wall and the first minimum (which we call the *first liquid layer*). Figure 1(a) (gray) further reveals that the mean mass flux toward the wall is correlated with the liquid density and thus exhibits a bottleneck at heights at which the liquid density is low. Because of the slower than average interchange of mass between the first liquid layer and the overlying bulk liquid, we assume that the liquid molecules in the first liquid layer reside long enough near the wall to justify a *dynamical* description of their molecular motion. Nonetheless, the wall-normal flux, indicating an

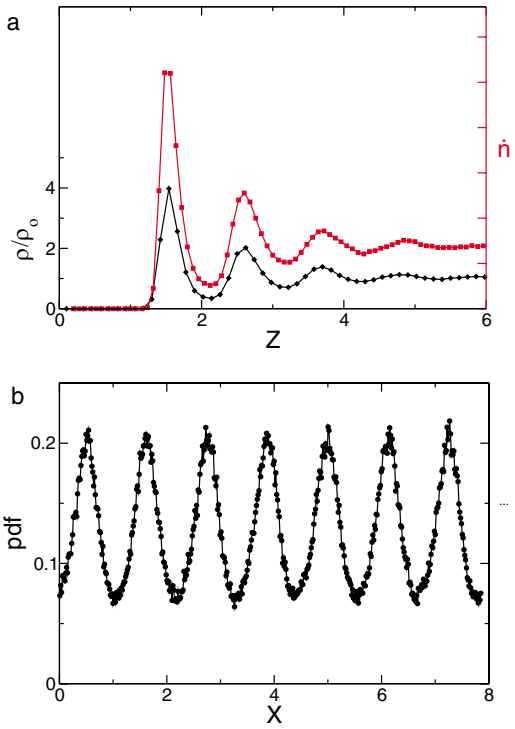

FIG. 1 (color online). MD simulations reveal that liquid near a wall is organized. (a) The mean mass flux $\dot{n}$ toward the wall (gray, red online) is correlated with the mean liquid density ρ (black) (normalized by the bulk density ρ_0). (To satisfy conservation of mass, the mean mass flux away from the wall follows precisely the same curve.) Z is distance from the wall, where the topmost layer of solid molecules is centered at $Z = 0$. (b) The probability density function (pdf) of the molecules in the first liquid layer as a function of distance X along the wall, for low forcing. Molecules spend most of their time positioned in the potential wells between the solid molecules. MD simulations conducted for this work are 2D. Renormalization of the liquid velocities (thermostatting) was not required: heat flows to the walls where it is removed [13].

interchange of molecules in the first liquid layer with those in the overlying liquid, must be taken into account. This introduces a stochastic component to our dynamical model as described below.

The dynamics of the first liquid layer is determined by the liquid-liquid and liquid-solid potentials, and energy exchange of the liquid with both the solid and the overlying bulk liquid. For simplicity we take the liquid-liquid potential to be quadratic $(K/2)(x_{i+1} - x_i - b)^2$ where b is the equilibrium spacing between liquid molecules and x_i is the position of the ith molecule along the interface. For a crystalline solid with lattice spacing λ, the potential φ above the solid can be written as a Fourier series [11] which we truncate after the first two terms, yielding $\varphi = h(1 - \cos 2\pi x_i/\lambda)$ where h is the strength of the potential. Both h and K can be related to parameters describing more realistic potentials, e.g., Lennard-Jones interactions used in our MD simulations. Momentum transfer $\eta_{ll}\dot{\gamma}_l$ from the bulk liquid is taken to be proportional to the instantaneous shear rate $\dot{\gamma}_l = (V - \dot{x}_i)/\delta$ where δ is the mean spacing between the first liquid layer and the layer above it moving at mean velocity V. η_{ll} is a coefficient of bulk viscosity. Momentum transfer to the wall occurs through an effective friction coefficient η_{ls} [4]. From the potentials and the momentum transfer terms, the equation of motion for the ith molecule, after applying the length and time scales $\lambda/2\pi$ and $\lambda m^{1/2}(2\pi h^{1/2})^{-1}$, is

$$\ddot{x}_i = -\sin x_i + k\,\triangle^{\dagger}\triangle x_i + f - \eta\dot{x}_i, \qquad i = 1, \ldots, N, \tag{1}$$

where k is the strength of the liquid-liquid coupling relative to the liquid-solid coupling, and f is the strength of the forcing due from the bulk liquid. f also contains a Gaussian random noise term to model deviations from the mean of the momentum transfer. The discrete diffusion operator has been introduced $\triangle^{\dagger}\triangle x_i = x_{i+1} - 2x_i + x_{i-1}$, η is a coefficient of viscosity assumed >1, and N is the number of molecules in the first liquid layer. In application, the parameters k and η would be chosen according to the properties of a particular liquid and solid. Equation (1) with fixed N is the damped, driven Frenkel-Kontorova (FK) equation [12]. Accounting for the wall-normal flux introduces a crucial modification: the number of molecules in the first liquid layer *fluctuates* in time,

$$N = N(t). \tag{2}$$

Because of the interchange of molecules between the first liquid layer and the bulk, all the molecules in the first liquid layer are ultimately replaced. We call (1) plus (2) the variable-density Frenkel-Kontorova model (vdFK). We specify $N(t)$ by considering that in the time interval dt, an additional molecule is added to or removed from the set N at a random location with probability $p_+ dt$ and $p_- dt$, respectively, where

$$p_+ = p + \alpha[s - a]_+, \qquad p_- = p + \alpha[a - s]_+. \tag{3}$$

p is a constant, $[g]_+ = g$ for $g > 0$ and is zero otherwise, and a and s are, respectively, the accumulated number of molecules added and subtracted to the ground state. Equation (3) is a simple rule which incorporates, through the term proportional to α, the experimental observation that, along an interface of fixed length C, there is a certain number of liquid molecules which is energetically preferred; see Fig. 1(b). Analogously, there is a preferred value of the ratio of the liquid-liquid to solid-solid spacings, $\xi = b/\lambda$, called the *ground state* that depends on the choice of solid and liquid. For example, $\xi = 1$ indicates that the state in which one liquid molecule sits in each potential well of the underlying substrate is preferred.

We solve (1) and (3) numerically to find the molecular velocities $\dot{x}_i(t)$ and positions $x_i(t)$ as a function of time [13]. The time average over all $N(t)$ molecular velocities $\dot{x}_i(t)$ yields v_s, the velocity at which the liquid slips relative to the solid. One result that requires no computation is apparent from the term f in (1) which, when restored to its dimensional form, is proportional to the bulk viscosity η_{ll}. Hence, the slip length (defined below) is predicted to increase with increasing viscosity. This counterintuitive result agrees with experiment [3].

Slip length $L_s = v_s/\dot{\gamma}$ is a common measure of the amount of slip. For convenience, we use

$$L_s = v_s/f \tag{4}$$

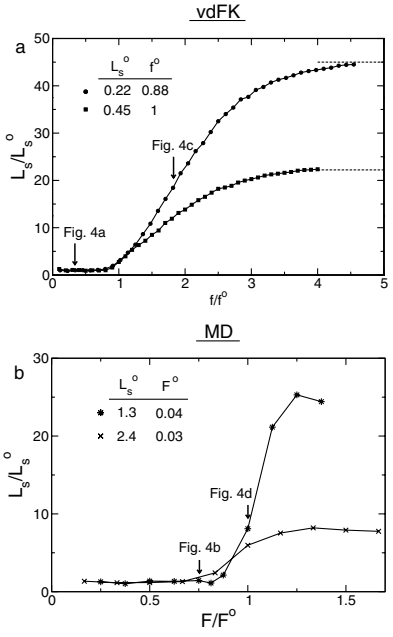

FIG. 2. Slip length L_s as a function of forcing for the vdFK model and MD simulations. At low levels of forcing, slip length is constant; there follows an abrupt increase in slip length and a leveling off at higher forcing. Results are normalized so as to collapse the low-forcing portion of the curves.

as the force, rather than the shear rate, which is the control parameter in (1). The MD simulations show that the fluid viscosity is constant [13], so the two definitions are proportional. The vdFK yields the characteristic slip curve as observed in MD simulation; namely, the slip length is constant at low-forcing followed by an increase of slip length [7], Fig. 2. (Furthermore, the vdFK model provides a dynamical explanation for this; see below.) Our MD simulations reveal a leveling off of slip length at high forcing as well, also borne out in vdFK simulations [13].

As the vdFK model provides a theoretical description of liquid motion on a *molecular scale*, it makes predictions of the dynamical states of the molecules themselves. There is a large body of work on the FK model, many results of which can be extended to the vdFK with some modification [12,14]. For fixed k and η those dynamical regimes seen in the FK model (i.e., for fixed N), which remain relevant for the vdFK model, as a function of the forcing f and the ground state ξ are as follows. Case (i): For ξ an integer the molecules are immobile until a critical forcing f_{SN} is reached [in (1) $f_{\mathrm{SN}} = 1$], at which point a saddle-node (SN) bifurcation to concurrent slip of the entire layer occurs. Case (ii): For ξ near an integer, e.g., $\xi = 99/100$ (i.e., one extra molecule per 100 periods of the substrate), the molecules act almost everywhere as in the integer case, with the exception of localized deformations, denoted *defects* or solitons [12,15]. As f is increased from 0, from an initially immobile ground state (now more complex topologically) there is a SN bifurcation to defect motion at $f_{\mathrm{PN}} = E_{\mathrm{PN}}(f)/\lambda$, where E_{PN} is the Peierls-Nabarro energy barrier to defect motion. The secondary SN bifurcation to concurrent slip of the entire layer persists at f_{SN}. Case (iii): For ξ sufficiently far from an integer value (or analogously for a density of defects large enough that the individual defects can no longer longer be discerned from one another) there is a SN bifurcation to concurrent slip already below f_{SN}.

The steady-state velocity of molecules obeying the FK equation as a function of ξ and f can be written $v_s(\xi, f)$ and has been determined for all three of the above-mentioned cases, both numerically and analytically where exact or perturbative methods can be applied. In particular, much is known about the velocity of isolated defects $v_d(f)$ in case (ii) [especially in the continuum limit of (1), the sine-Gordon equation] and the velocity of the molecules in case (iii) is described by the dynamic Hull function $v_h(\xi, f)$ [16].

The effect of the introduction of (2) can therefore be approximated by the FK equation in the adiabatic limit in which changes in $N(t)$ are slow. In this case ξ also changes slowly and the instantaneous slip velocity is approximated well by $v_s(\xi(t), f)$. Thus, for example, cases (i) and (ii) both yield $v_s(\xi(t), f) = (N(t) - N_0)v_d(f)$ (for $f < f_{\mathrm{SN}}$), where N_0 is the number of molecules for which ξ is an integer. That is, the degree of slip is proportional to the number of defects (for a fixed domain C). The time average of the instantaneous slip $\langle v \rangle = T^{-1} \int_0^T dt v_s(\xi(t), f)$ yields an approximate slip velocity, which for weakly interacting defects reduces to $\langle v \rangle = n v_d$, where $n = \langle N(t) - N_0 \rangle$ is the average number of defects. Together with the continuum limit of (1) [17],

$$v_d \sim k^{1/2} f \quad \text{as } f \to 0, \tag{5}$$

$\langle v \rangle$ yields an approximation to v_s good until the onset of concurrent slip, Fig. 3. Moreover, from (3), n is independent of the amplitude of forcing, so $v_s \cong \langle v \rangle \propto k^{1/2} f$. Using this expression in (4) yields $L_s \propto k^{1/2}$. Recalling that k is the ratio of the strength of the liquid-liquid to liquid-solid coupling, this expression agrees with the observation that more strongly nonwetting (larger k) liquids have larger slip lengths [18]. Furthermore, note that slip due to defects leads naturally to a force-independent L_s, as characteristically observed at low forcing, e.g., Fig. 2. How rapidly $N(t)$ changes depends on (3), and the above approximations become exact only for $p, \alpha \to 0$. In general, as p and α increase in magnitude, transients become important and the above argument breaks down.

A very strong prediction of the vdFK model is that given a ground state ξ, which is near an integer value, two distinct slip mechanisms should be observed. Specifically, for $f_{\mathrm{PN}} < f < f_{\mathrm{SN}}$ slip occurs due to localized defects, generated at a rate given by the wall-normal flux, Fig. 4(a). For $f > f_{\mathrm{SN}}$ the shear at the interface is sufficient to move large domains of molecules concurrently, Fig. 4(c). In order to compare these vdFK predictions with MD experiments, we extract MD trajectories as follows: (i) the first liquid layer is defined from the density profile [e.g., see Fig. 1(a)]; (ii) molecules within this layer are instantaneously identified; (iii) the x position of this set of molecules is determined. Steps (ii) and (iii) are repeated at each time step.

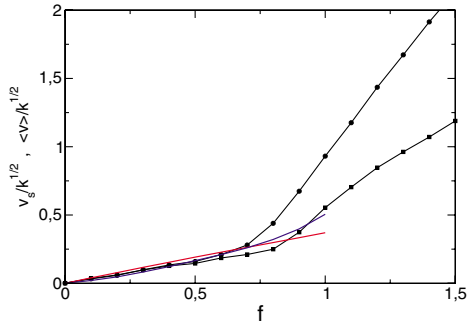

FIG. 3 (color online). At low forcing, the slip velocity v_s measured by averaging over the molecules in the first wall layer is well approximated by the speed of an individual defect times the average number of defects [$\langle v \rangle$, $k = 0.3, 1.0$ (blue and red online, respectively)]. The defect approximation breaks down at $f_{\mathrm{SN}} \approx 1$ due to the onset of concurrent slip.

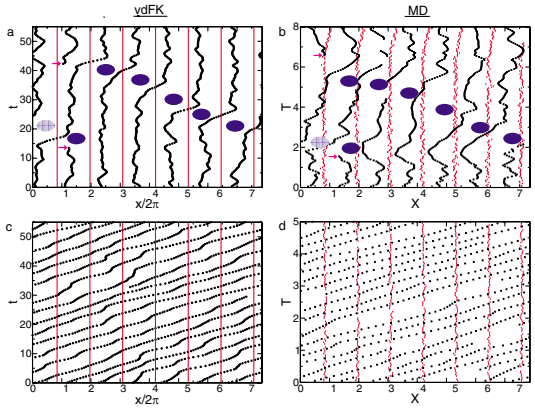

FIG. 4 (color online). Molecular trajectories predicted by the vdFK (left column) and from MD experiments (right column). The top two figures are at low forcing; the bottom two are at high forcing. Time increases upward from the bottom of each panel. The frame of reference is fixed with the wall. The trajectories are composed of closely spaced black dots marking the positions $x_i(t)$. When a liquid molecule leaves to (arrives from) the bulk, its trajectory ends (appears). The positions of the seven solid molecules on the surface of the wall appear as vertical lines. As an aid to the eye, a potential well with no liquid molecule is marked by an oval. (a),(b) Initially, all wells are occupied ($\xi = 1$) and there is no slip. A molecule departs (lower arrow) generating a vacancy which propagates upstream until another molecule arrives (upper arrow), filling the vacancy, and restoring the defect-free state and no slip. (c),(d) For larger forcing, defect slip is overwhelmed by the translation of the entire liquid layer.

Figure 4 provides a comparison of the defect- and concurrent-slip regimes in the vdKF predictions and in MD simulations and reveals a striking qualitative agreement in behavior. Furthermore, in the MD simulations, the defect-driven slip is observed throughout the region of constant slip length for low forcing, while concurrent slip is seen during and beyond the dramatic increase in slip length at higher forcing, as predicted by the vdFK.

The vdFK model thus appears to capture the distinct dynamical mechanisms which lead to liquid slip, at least in MD simulations. This also shows, *a posteriori,* that it is indeed possible to describe the phenomenon of liquid slip via a dynamical description of the molecular motion of the liquid layer adjacent to the interface alone.

There has been some debate as to whether slip occurs at all forcing levels or if a minimum forcing is required in order for slip to commence. The vdFK model suggests that either is possible. For the parameter values chosen here, f_{PN} is too small to be discerned in Fig. 2. However, for other parameter values (not shown) f_{PN} is discernible, as is observed in experiment [3].

The FK equation was first introduced as a model of dislocation motion in solids [12]. So, it may seem surprising that the vdFK equation successfully models liquid dynamics at the liquid-solid interface. However, the FK equation treats closed systems, while the vdFK models open systems. The first liquid layer is solidlike on short-time scales [as described by FK dynamics, (1)]. On longer scales, flux into and out of the layer generates the molecular interchange characteristic of liquids [as described by the variable-density equation, (2)]. At low forcing levels, the mean density of solitons is determined by the wall-normal flux of liquid molecules. If the soliton velocity can then be calculated based on the liquid-wall properties, the slip is known. The combination of short-time-scale order plus long-time-scale loss of molecular identity is required to describe liquid slip along solid surfaces.

This research is funded by the National Science Foundation SGER DMS-0200762 and DGE-9987577. We thank Pulak Dutta, GertJan van Heijst, Joel Koplik, Julio Ottino, and Mike Peshkin for useful discussions.

[1] M. Navier, Mém. l'Acad. Sci. **6**, 389 (1823).
[2] A. Karlsson *et al.*, Nature (London) **409**, 150 (2001); P. Ball, Nature (London) **423**, 25 (2003).
[3] V. S. J. Craig, C. Neto, and D. R. M. Williams, Phys. Rev. Lett. **87**, 054504 (2001); Y. Zhu and S. Granick, Phys. Rev. Lett. **87**, 096105 (2001); E. Bonaccurso, M. Kappl, and H.-J. Butt, Phys. Rev. Lett. **88**, 076103 (2002).
[4] R. Pit, H. Hervet, and L. Léger, Phys. Rev. Lett. **85**, 980 (2000).
[5] L. Léger, J. Phys. Condens. Matter **15**, S19 (2003).
[6] J. Koplik, J. R. Banavar, and J. F. Willemsen, Phys. Fluids A **1**, 781 (1989).
[7] P. A. Thompson and S. M. Troian, Nature (London) **389**, 360 (1997).
[8] J.-L. Barrat and L. Bocquet, Phys. Rev. Lett. **82**, 4671 (1999); S. Granick, Y. Zhu, and H. Lee , Nature Mater. **2**, 221 (2003).
[9] C.-J. Yu *et al.*, Phys. Rev. Lett. **82**, 2326 (1999); J. N. Israelachvili, P. M. McGuiggan, and A. M. Homola, Science **240**, 189 (1988); F. Heslot, N. Fraysse, and A. M. Cazabat, Nature (London) **338**, 640 (1989).
[10] P. A. Thompson and M. O. Robbins, Phys. Rev. A **41**, 6830 (1990).
[11] W. A. Steele, Surf. Sci. **36**, 317 (1973).
[12] O. M. Braun and Y. S. Kivshar, Phys. Rep. **306**, 1 (1998).
[13] See EPAPS Document No. E-PRLTAO-93-053433 for molecular dynamics simulations. A direct link to this document may be found in the online article's HTML reference section. The document may also be reached via the EPAPS homepage (http://www.aip.org/pubservs/epaps.html) or from ftp.aip.org in the directory /epaps/. See the EPAPS homepage for more information.
[14] L. M. Floría and J. J. Mazo, Adv. Phys. **45**, 505 (1996).
[15] F. C. Frank and J. H. van der Merwe, Proc. R. Soc. London A **198**, 205 (1949).
[16] T. Strunz and F.-J. Elmer, Phys. Rev. E **58**, 1601 (1998).
[17] F. G. Bass *et al.*, Phys. Rep. **157**, 63 (1988); Y. S. Kivshar and B. A. Malomed, Rev. Mod. Phys. **61**, 763 (1989).
[18] J.-H. J. Cho *et al.*, Phys. Rev. Lett. **92**, 166102 (2004).